Ocean Modelling 184 (2023) 102210

Contents lists available at ScienceDirect

Ocean Modelling

journal homepage: www.elsevier.com/locate/ocemod

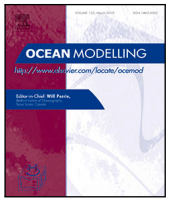

HyWaves: Hybrid downscaling of multimodal wave spectra to nearshore areas

Alba Ricondo [a,*], Laura Cagigal [a], Ana Rueda [a], Ron Hoeke [b], Curt D. Storlazzi [c], Fernando J. Méndez [a]

[a] Geomatics and Ocean Engineering Group. Departamento de Ciencias y Técnicas del Agua y del Medio Ambiente. E.T.S.I.C.C.P. Universidad de Cantabria, Santander, Spain
[b] Commonwealth Scientific and Industrial Research Organization (CSIRO), Oceans and Atmosphere, Aspendale, Australia
[c] Pacific Coastal and Marine Science Center, United States Geological Survey (USGS), Santa Cruz, United States

ARTICLE INFO

Keywords:
Hybrid downscaling
Data mining
Multimodal wave climate
Spectral partitioning
Directional wave spectra

ABSTRACT

Long-term and accurate wave hindcast databases are often required in different coastal engineering projects. The assessment of the nearshore wave climate is often accomplished by using downscaling techniques to translate offshore waves to coastal areas. However, dynamical downscaling approaches may incur huge computational cost. Additionally, the common use of bulk parameterizations are often not accurate for multidimensional waves. To overcome these limitations, we present a hybrid downscaling approach that combines mathematical algorithms (statistical downscaling) and numerical modeling (dynamical downscaling) over the individual spectral partitions. Every wave partition is downscaled and aggregated afterward by using principles of wave linear theory. By assuming linearity in the propagation of the wave celerity, the application of the method is limited from offshore to intermediate water depths. In addition, the method proposed uses a technique to simplify the spectral boundary conditions in complex domains. The methodology has been applied and validated in the island states of Samoa, American Samoa, Majuro, and Kwajalein, showing good skill at reproducing the spectral hourly time series of significant wave height, peak period, and peak direction. Moreover, an accurate representation of the observed energy spectrum was achieved. This study provides insight into the numerical approximation of the combined sea-swell states while improving the quality of fast spectral forecasting and early warning systems.

1. Introduction

Downscaling of long-term series of local wave climates is essential for many engineering activities related to ocean and coastal management (e.g., design of coastal protection, analysis of wave resonance in harbors, or the study of morphological evolution on beaches). Similarly, forecasting local wave conditions is an essential input into coastal hazard Early Warning Systems (EWS). At present, the development of accurate and efficient EWS to forecast short-term coastal hazards is necessary to provide local risk managers with adequate tools to anticipate severe coastal damages and reduce the vulnerability of coastal communities. One of the advances needed in the development of EWS is the improvement of downscaling techniques for offshore waves (Wandres et al., 2020; Winter et al., 2020). The most widely utilized wave transfer method is dynamic downscaling with third-generation spectral wave models. However, this solution is often not practical due to computational resource constraints (Camus et al., 2011a,b). As an alternative, hybrid and/or statistical downscaling techniques have been developed as computationally efficient complements to numerical models (Camus et al., 2014; Cid et al., 2017), with a wide variety of wave transformation metamodels (Camus et al., 2013; Gouldby et al., 2014; Rajindas and Shashikala, 2021). These methods, however, lose information on the full wave spectrum since they focus on the integral parameters of the spectra (i.e. bulk wave statistics such as significant wave height, mean period, and mean direction), which are frequently used in engineering projects (Gerling, 1991). Additionally, in locations with complex bathymetry and multimodal wave conditions, as is typical for islands located in large ocean basins, it is crucial to avoid the integral properties of the spectra as they may inadequately solve the spectral transformation to the coast (Draycott et al., 2017). Although recent studies have already made use of spectral partitioning algorithms in statistical downscaling approaches (Anderson et al., 2021; Hegermiller et al., 2017), they use a limited number of spectral partitions. To overcome these limitations, we present an adapted hybrid method capable of downscaling complex hindcast or forecast wave conditions in a highly computationally efficient manner.

* Corresponding author.
E-mail address: ricondoa@unican.es (A. Ricondo).

https://doi.org/10.1016/j.ocemod.2023.102210
Received 24 January 2023; Received in revised form 3 May 2023; Accepted 11 May 2023
Available online 15 May 2023

Table 1
Location, anchoring depth, and measurement period of the sensors used for validation off Pacific Islands.

Site	Lon (°)	Lat (°)	Depth (m)	Start	End
Majuro	171.4016	7.0891	375	24 April 2010	19 January 2015
	171.3918	7.0835	540	4 May 2016	Present
Roi-Namur	167.4678	9.4074	21	3 November 2013	4 April 2015
Kwajalein	167.7000	8.7200	11	9 November 2013	10 April 2015
Samoa	188.7800	−14.4150	80	1 September 1989	11 April 1990
American Samoa	189.5070	−14.2650	75	23 October 2014	30 May 2018
	189.4995	−14.2732	55	30 May 2018	Present

The methodology presented in this paper henceforth referred to as HyWaves (Hybrid Waves) aims at providing a rapid and robust technique to include spectral and directional complexity when downscaling multi-modal wave climate to coastal areas. Here we propose an efficient wave-modeling tool supported by clustering and interpolation techniques to overcome computational constraints and ease the integration of long-term coastal hazards and future climate change scenarios for comprehensive coastal risk assessments. We present its application and validation to multiple Pacific Island sites. Such locations are especially challenging to downscale due to the frequent existence of multiple swell and wind-sea systems at any given time, combined (typically) with steep, complex, and rugous surrounding reef systems that modify the incoming wave fields in complex ways due to refraction and dissipation.

The paper is structured as follows: Section 2 presents the study sites and observational datasets collected. Section 3 describes the methodology in detail with five subsections "Energy aggregation: Super-point", "Super-point partitioning and rescaling", "Selection", "Dynamical downscaling" and "Wave systems reconstruction and aggregation". The validation of the metamodel is given in Section 4, while conclusions are covered in Section 5.

2. Study sites and data

HyWaves methodology has been applied and validated in several Pacific Island nations (i.e., Majuro and Kwajalein Atolls in the Marshall Islands in the north Pacific, and Samoa and Tutuila Island in the South Pacific). These low-lying tropical coral reef-lined coasts and atoll islands are exposed to distant north and south Pacific storm swells mostly generated during their respective winter seasons (Genz et al., 2009). Out of the several wave-driven flooding hazards that threaten these coastal areas (e.g., tropical storms, typhoons, ENSO events) (Ford et al., 2018), the episodes of flooding due to the dissipation of far swell fields are frequently overlooked (Hoeke et al., 2013, 2021). However, infragravity waves released from the breaking of long-crested waves along the coral reef shoreline, generally when combined with high-tides, have a strong potential to cause overwashing.

In Kwajalein Atoll, HyWaves has been tested in two locations, Roi-Namur at the northern point and Kwajalein at the southern point. In Roi-Namur, a 0.5 m resolution bathymetric digital elevation model (Storlazzi et al., 2018) was used, and a 10 m resolution topo bathymetry from United States Army Corps Engineers (USACE) for the Kwajalein site. In Majuro Atoll, a 1-meter topobathymetric digital elevation model was used, available at the United States Geological Survey (USGS) (Palaseanu-Lovejoy et al., 2018). Gaps in the bathymetry were filled in both domains with 0.42^{o} resolution data from the General Bathymetric Chart of the Oceans (GEBCO).

In-situ data was collected for both Kwajalein Atoll deployments with bottom-mounted pressure loggers from a geophysical survey carried out by Rosenberger et al. (2020). The data used at the southern location was collected by a Virtuoso Dwave sensor in two separate periods (9 November 2013 to 19 April 2014; 30 October 2014 to 10 April 2015). Data in the northern location, in Roi-Namur, were measured by a 600 kHz Nortek Acoustic Wave and Current Meter (AWAC) placed on the fore reef as described in Cheriton et al. (2016) and collected in three separate periods (3 November 2013 to 13 April 2014; 29 April 2014 to 6 October 2014; and 25 October 2014 to 4 April 2015). In Majuro, the buoy employed is a Datawell Directional Waverider Mark III (DWR-MkIII) owned and managed by the Pacific Islands Ocean Observing System (PACIOOS) and collects data every half an hour with a measuring period from 24 April 2010 to the present. Details on the location of the buoys are given in Table 1.

For brevity, hereafter we focus on the application of the method to the Samoa and American Samoa sites and omit the details of the Marshall Islands sites, but the treatment is the same at all sites. The Samoa Islands consist of Savai'i and Upolu, and on the western archipelago of American Samoa, Tutuila Island is also addressed. Bathymetric data have been obtained by combining two data sources. At the regional scale of Samoa and Tutuila Island, the bathymetry used has been produced by blending GEBCO, Smith and Sandwell (1997) bathymetry, and nearshore multibeam echosounder bathymetry gridded at 250 m resolution (Kruger, 2007). A finer bathymetry of Tutuila Island has been embedded, providing a complete bottom coverage at a 5 m grid resolution extending to 250 m depth, available from the Pacific Islands Benthic Habitat Mapping Center (http://soest.hawaii.edu/pibhmc). The merged bathymetries are shown in Fig. 1a.

Finally, the validation was undertaken using in-situ wave measurements from both a bulk (non-directional) wave buoy located between Savai'i and Upolu and a spectral wave buoy located 7 km offshore the eastern shore of Tutuila Island, close to the small volcanic island of Aunu'u. The non-directional Waverider buoy was located close to Apolima Island and moored at 104 m depth. The buoy was part of the South Pacific Applied Geoscience Commission (SOPAC) wave data collection program aiming at mapping the wave energy of South Pacific Island nations. With a relatively short collection period (1 September 1989–11 April 1990), the buoy was exposed to the passage of Cyclone Ofa on 4 February 1990, to Tropical Cyclone Rae on 26 March 1990 and to south swells and trade winds (see details in Barstow and Haug, 1994). The mean significant wave height (H_s) recorded by the buoy was 1.5 m with a mean peak wave period (T_p) of 10 s. However, the buoy also measured extreme wave events of H_s up to 10 m or T_p up to 22 s.

The spectral Aunu'u buoy is also a DWR-MkIII owned and managed by the Pacific Islands Ocean Observing System (PACIOOS). Moored at 55 m depth, it collects data every half an hour from 23 October 2014 to the present. Normal conditions range from calm ($H_s < 2$ m), to typical moderate wave events ($H_s = 4$–5 m), to energetic wave events ($H_s > 4$ m), as demonstrated in Fig. 1c. The longest period swells approach the island from the northern and southern hemispheres with H_s between 2–3 m and periods between 20–22 s. Eastern trade winds are constantly blowing over the area resulting in events with H_s up to 4 m and $T_p \sim 12$ s.

Spectral wave data corresponds to the CAWCR wave hindcast 1979–2022 produced by the Bureau of Meteorology and CSIRO (Smith et al., 2020). The database comes from the WAVEWATCH III version 4.08 numerical wave model, with 0.4^{o} global grid spacing and a series of nested regional grids with 4 arc-minute (approximately 7 km) spatial resolution, including around the Pacific islands. The wave hindcast is forced with hourly surface winds from the Climate Forecast System Reanalysis (CFSR) (Saha et al., 2010) and CFSv2 Reanalysis (Saha et al., 2011) generated by the National Center for Environment Prediction

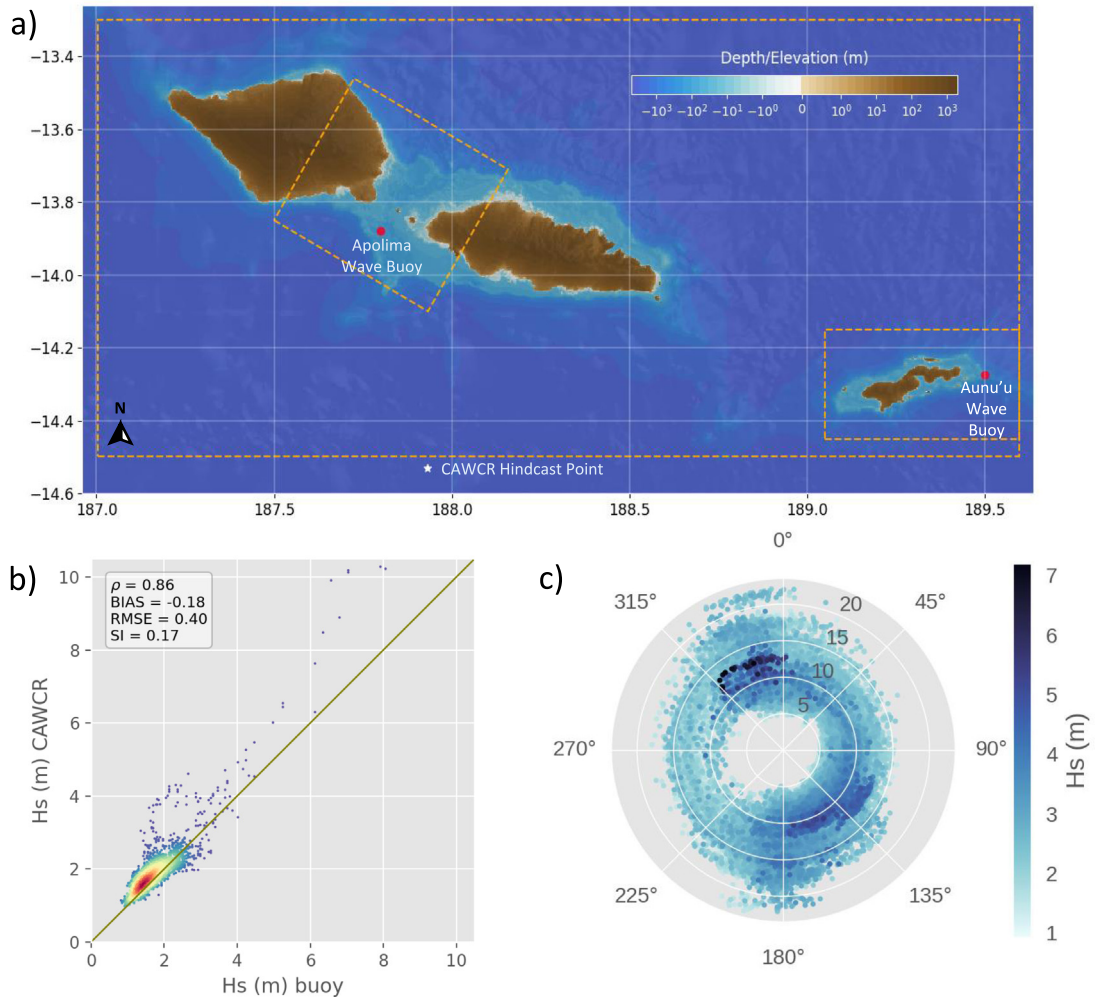

Fig. 1. Bathymetry and buoy data for the Samoan Islands. (a) SWAN computational grids (in dashed orange boxes) and bathymetry of Samoa and Tutuila used for the study. The red dots are the locations of the Apolima buoy and the Aunu'u buoy. (b) Density scatter of the H_s measured by the Apolima Buoy and the CAWCR hindcast point (white star in (a)). (c) Hourly sea-states retrieved by the Aunu'u buoy. The radial axis corresponds to T_p and colored points indicate the H_s of the event.

(NCEP). In addition to gridded integrated wave parameter and partition parameter output, hourly wave spectra discretized into 24 directional and 29 frequency bins ranging from 0.0345 to 0.5476 Hz is available at discrete locations. The comparison between the H_s measured by the Apolima buoy and the H_s provided by the CAWCR hindcast point located in southern Samoa is provided in Fig. 1a. Due to the inadequate representation of the bathymetry, the hindcast has significantly less energy than the buoy. This reinforces the need for a high-resolution downscaling and calibration of the global wave hindcast.

3. Methodology

A schematic of the methodological framework is displayed in Fig. 2; the details are described in the following sub-sections. HyWaves is based on the use of a statistical-dynamical hybrid model to transfer offshore multimodal wave climate to the coast with minimal computational effort. First, the boundary conditions for the dynamical downscaling are generated considering the convolution of the spectral data from the 43-year CAWCR hindcast stations into a "Super-point" (Section 3.1). The spectral information is condensed and parameterized into the wave partitions (Section 3.2), which are the input to HyWaves. The metamodel is built up by the selection of representative cases with the Maximum-Dissimilarity Algorithm (MDA) (Section 3.3); these cases are dynamically (numerically) modeled using SWAN (Simulating Waves till Nearshore) (Booij et al., 1999) (Section 3.4); and the reconstruction using the Radial Basis Functions (RBF) interpolation technique (Section 3.5). Finally, the original record is reconstructed at certain locations by linearly aggregating the different concurrent wave systems (Section 3.5).

3.1. Energy aggregation: Super-point

Cagigal et al. (2021) first introduced the concept of "Super-point" as a practical way to aggregate spectral wave information and create a unique time series of the incoming wave energy to an island. The same approach is used in this work as the input to the numerical (dynamical) downscaling, thus simplifying the library of cases to be run by the metamodel. The available CAWCR spectral points around Samoa and Tutuila Island are shown in Fig. 3. The "Super-point" construction is then built hourly on the angular sectors that receive the incoming energy from each hindcast point. Note that for the 15 available points, a sector of 24º will be taken, except for the 2 points in the northeast corner, which will each represent 36º. By doing this, the Super-point aggregates all the incoming energy into a single spectrum that represents the complexity of the multimodal directional spectrum. An example of Super-point construction for 19 October 1987 at 01:00

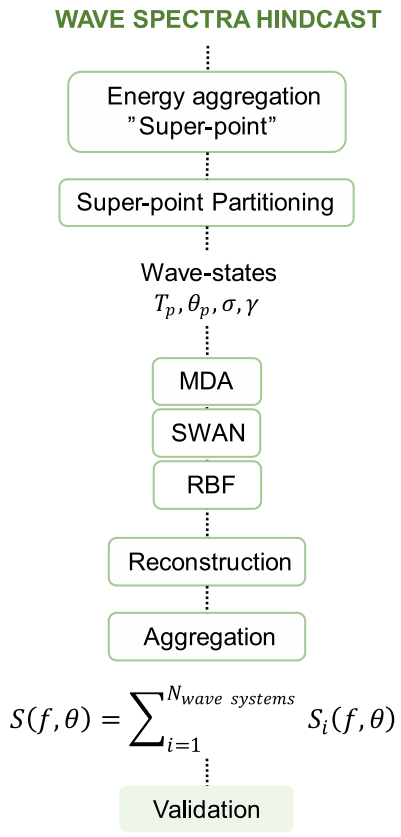

Fig. 2. Schematic of the HyWaves methodological framework for downscaling multimodal wave systems.

a.m., which is representative of common wave and wind condition, is presented in Fig. 3b.

3.2. Super-point partitioning and rescaling

Applying the MDA selection algorithm over the full spectrum would be impractical to manage. A well-known data reduction technique consists of obtaining the integral parameters of the spectrum. However, in complex coastal settings, where wave propagation is highly sensitive to spectral shape and directional properties, a more complete characterization of the spectra is desired to prevent unrealistic numerical results. To accomplish this, the Super-point spectrum is decomposed into the individual wind sea and swell systems. The spectral partitioning technique, first introduced by Gerling (1992) and further enlarged by Hanson and Phillips (2001) and Portilla et al. (2009), establishes a method to track the temporal evolution of spectral components. Here, we use the Wavespectra package (https://github.com/metocean/wavespectra), which implements the watershed partitioning of Hanson and Phillips (2001). The algorithm is based on a topographical minima criterion applied to recognize the peaks within the two-dimensional spectrum. The local wind sea is identified based on the phase speed of the wind sea, the 10-m elevation wind speed, and the angle between the wind and the wind sea. After removing partitions with low energy and combining those with closely spaced spectral locations, the algorithm considers the remaining wave peaks as swells. For this analysis, the algorithm is set up to identify a maximum of five swells. An example partitioned sea surface spectrum of the Super-point instant is illustrated in Fig. 3b. The partitions, delimited by different colormaps, exhibit six wave systems: one swell coming from the south and one from the north, two from the northwest, one from the northeast, and a wind-sea coming from the east-southeast. The orange arrow indicates the peak wind direction, corresponding to 130º and a wind speed of 5 m/s.

Table 2
Parameterization of the wave systems present in the Super-point composition at a given time (10 October 1987, 01:00 a.m.). Partition 1 to 5 correspond to swell systems, whereas partition 0 represents the local wind-sea component.

Partition	H_s	T_p	θ_p	σ	γ
0	1.13	8.7	112.5	23.2	1
1	0.69	11.8	217.5	8.5	9
2	0.59	14.2	217.5	10.9	100
3	0.59	10.1	7.5	9.3	60
4	0.35	11.1	187.5	1.2	74
5	0.3	8.1	37.5	12.7	15

The Wavespectra package also derives integral parameters (statistics) of each partition of the wave spectrum; this represents a considerable data reduction that preserves multi-modal directional information. The partitioned parameters are: H_s, T_p, peak wave direction (θ_p), directional spreading (σ), and JONSWAP peak-enhancement factor (γ). Since the present Wavespectra version (v3.6.1) does not compute the γ parameter, we calculate it by integrating the spectrum in frequencies and fitting it to a potential equation as in Cagigal et al. (2021). Although the JONSWAP formulation (Hasselmann et al., 1973) was originally proposed to describe partially developed spectra, it also fits narrow-band spectra, characteristic of swells out of the wind fetch (Goda, 1983). The γ parameter is constrained between 0 and 50 to stay within a numerically realistic range of values. As an illustration, the parameterization of the wave systems existent at the specific moment shown in the Super-point construction and partitioning (Fig. 3a, 3b, and 3c) is summarized in Table 2.

In the absence of wind or non-linear effects, the propagated and the initial H_s between two locations is directly proportional to a propagation coefficient (K_p). We define K_p as the rate at which wave amplitude changes as it propagates. This measure describes the attenuation or amplification during wave propagation. Following this principle, in deep waters, the propagated H_s for an initial H_s of 1 m will be directly the K_p and the propagated H_s for an initial H_s of 2 m is $2 \cdot K_p$. Therefore, we can replace every H_s value by 1 m and eventually rescale the resulting value. Note that for small T_p, this approach may create very steep waves. In order to prevent non-linearities of deformed waves, T_p smaller than 5 s are run with H_s equal to 0.1 m and T_p higher than 5 s with H_s equal to 1 m. This assumption reduces the dimensionality of the wave systems and allows direct visualization of the K_p.

Once the partitions have been identified, it is possible to show a new representation in the frequency-direction space, computed as the percentage of time in which the peak energy is located at specific bins. The probability occurrence of spectral peak positions allows greatly improved linkage of the wave systems with their generation regions (Portilla-Yandún et al., 2015). The occurrence distribution of bulk and partitioned peak wave systems, respectively, are presented in Fig. 3d and 3e. With bulk statistics (Fig. 3d), the peak energy appears condensed in the 80–130º sector, indicating that 18% of the time, energy is present in that sector. However, using partitioned statistics allows a more accurate description of wave energy. The probability of occurrence of wave systems demonstrates how swells in the 170º and 200º sectors are more likely to be encountered than wind-sea (Fig. 3e). These discrepancies highlight how bulk wave statistics are poorly fitted to the multimodality of the wave climate in Samoa and reaffirms the importance of avoiding bulk metrics in favor of the individual parameterization of spectral partitions.

3.3. Selection

To reduce the computational effort involved in dynamically downscaling the wave conditions to the coast, we make use of the selection MDA technique. This algorithm has been previously used in downscaling works (Camus et al., 2011a,b) to select representative sea-states

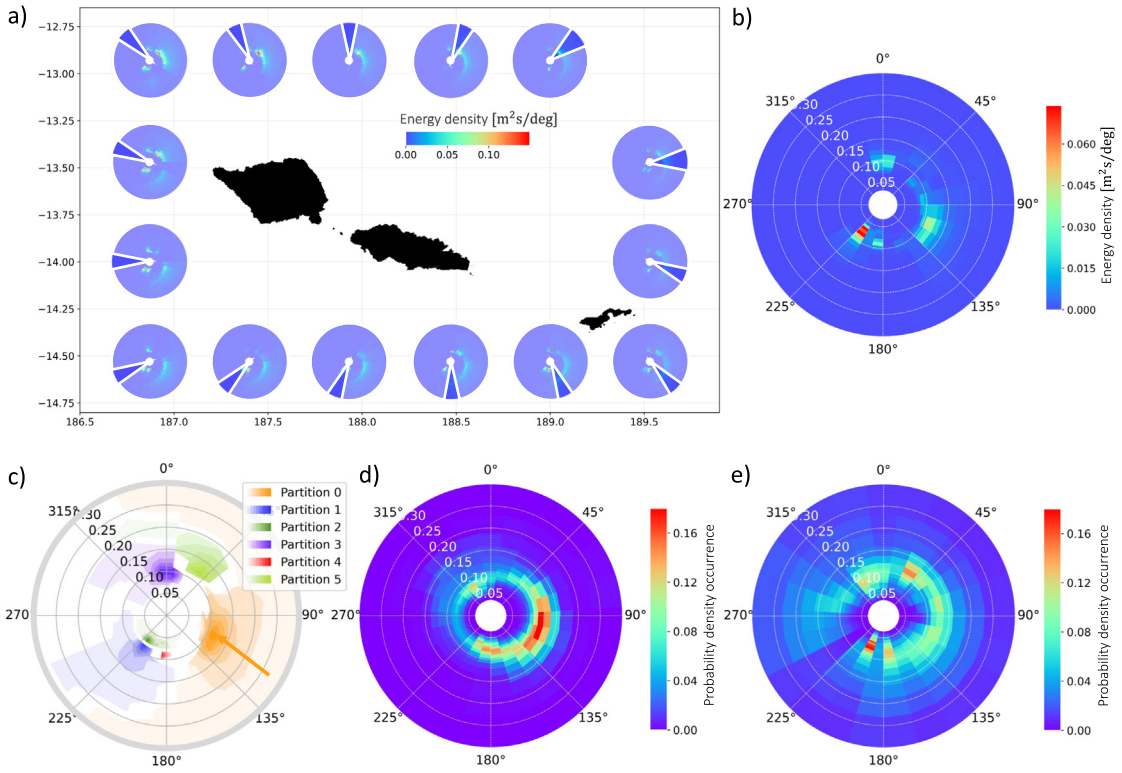

Fig. 3. Super-point definition. (a) Spectral stations around Samoa and Tutuila from the CAWCR wave hindcast. (b) "Super-point" creation from the stations in (a). (c) Wave systems found at the spectral instant in (b). The arrow indicates the direction of the wind vector. (d) Probability of occurrence of bulk peak parameters. (e) Probability of occurrence of peak spectral partitions. The direction in the spectra is the direction the waves are coming from; radial axis corresponds to frequency in hertz.

to construct a metamodel. In this research, the number of centroids (M cases) that adequately reproduce the singularity of the dataset were determined by a sensitivity analysis described in Section 3.5. Once the number of design cases is known, the MDA algorithm is implemented on the normalized data vectors, $X_i = T_p, \theta_p, \sigma, \gamma$ using a linear transformation that scales the scalar values between 0–1 and the directional variables (dividing by π) between 0 and 2. In n-dimensional space, the MDA identifies the subset cases iteratively. Distances are implemented by the Euclidean distance in the case of scalar variables and circular distances for directional variables. The algorithm seed corresponds to the most dissimilar case. Subsequently, the following subset case is calculated from the input data as the vector with the maximum distance to the seed. The algorithm finishes when the length of the subset reaches the desirable M cases. A more detailed description of the algorithm is given in Camus et al. (2011a,b). The subset cases distribution over the initial offshore conditions is shown in Fig. 4b. Subset cases cover the space uniformly, avoiding issues with densely populated areas and efficiently selecting extreme events.

3.4. Dynamical downscaling

At any time and position, the surface wave field can be reproduced as the sum of a large number of harmonic wave components (Holthuijsen, 2010). These components are expected to behave as linear waves, propagating out of their wind genesis with minimal interaction among their constituents. In their shoreward propagation, waves start interacting with bathymetry, where transformation processes such as wave refraction, shoaling, and surf breaking takes place. Due to the narrow reef flat and steep reef slope of these atolls, the bathymetry remains deep water until relatively close to shore. Consequently, we can use linear assumptions for the wave field, propagating the individual wave partitions of the spectra separately and aggregating them linearly at the target location. The numerical simulation of the M wave partitions selected by the MDA is performed using the SWAN wave model.

The computational grid schemes for Samoa and Tutuila Island are presented in Fig. 1a. A regular grid with a 1 km-wide cell is defined for both islands, extending 2.6° longitude and 1.2° latitude. To better downscale the CAWCR hindcast to the wave buoy locations, two nested higher-resolution grids were set up. A mesh with a grid resolution of 250 m was embedded between Savai'i and Upolu, containing the Apolima wave buoy. This mesh is 30º rotated to make the north contour perpendicular to the swell entrance. Finally, to improve the modeling of shoaling and wave refraction close to the shallow water around the Aunu'u buoy, a mesh with a resolution of 50 m was defined centered on Tutuila Island.

As input for the dynamical downscaling, the SWAN model is forced with hourly parametric wave conditions, constant along the boundaries. The tide level is set constant and equal to 0 and the simulation period to 1 hour, run in stationary mode. The model output data consists of the hourly parameters of H_s, T_p, T_m, θ_p, and σ. As the 800 subset cases were modeled in SWAN with H_s equal to 1 m, the outputted H_s corresponds to the K_p factor. Spatial fields of K_p, T_p and θ_p can be seen in the propagation of the first 25 MDA cases in Fig. 4c for the main mesh and Fig. 4d for the nested mesh in Tutuila Island. The cases would be further defined by the σ and γ parameters. Although these parameters provide additional valuable information about wave behavior, they have been omitted from the figure to keep it less complicated. The output propagations are arranged first horizontally and then vertically in the same sequence as the MDA selection. Therefore, the first propagation in the panel corresponds to the most extreme MDA condition, which has a T_p of 27 s. In deep waters, the most important variations in H_s and θ_p are induced by island shadowing phenomena (values smaller than 1 m). In the coastal areas of Tutuila Island, the longest periods leader to greater wave focusing and particularly wave shoaling, resulting in local enhancement of the energy (values larger than 1 m).

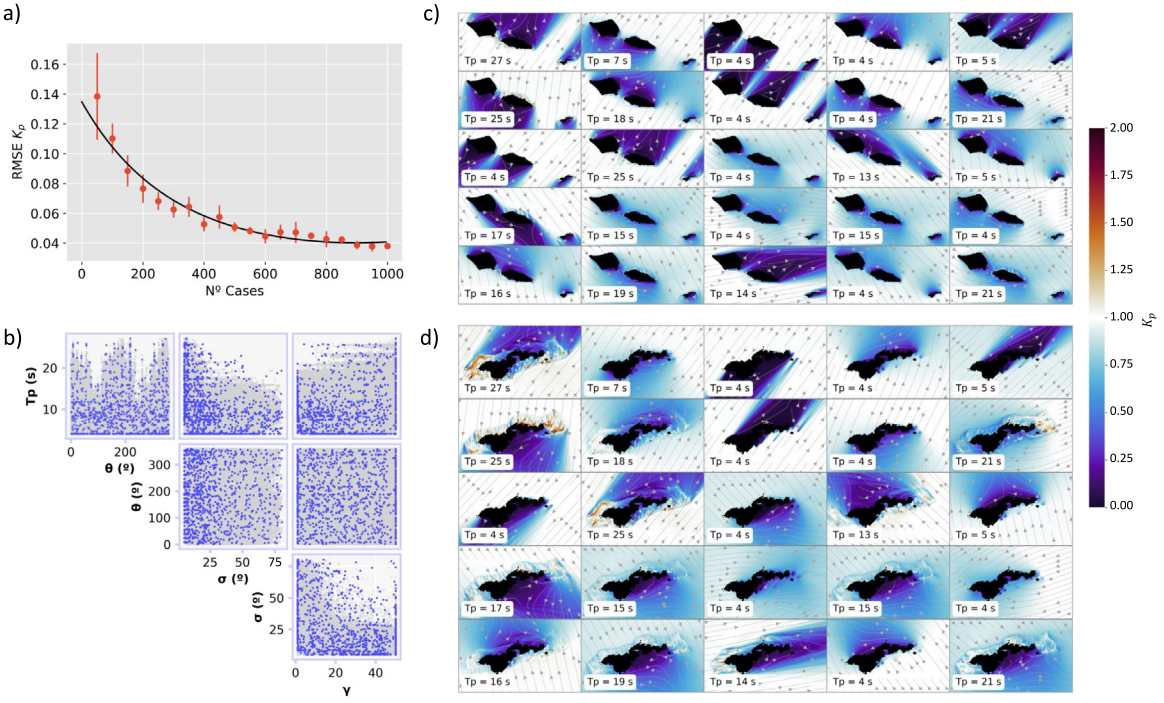

Fig. 4. MDA selection and numerical modeling. (a) Root-mean-square error of K_p as a function of the selected number of cases. The black line is the second-degree exponential fitting curve. (b) Multidimensional distribution of the MDA subset cases. The gray region delimits the input data vectors, while blue points represent the selected cases. (c) Propagation coefficient, peak direction, and peak period of the first 25 subset cases of the MDA-swells for the full Samoa SWAN grid. The T_p value is specified in the text box, K_p is denoted by the color, and θ_p is mapped using streamlines. (d) Same 25 MDA subset cases that in (c) modeled on the nested grid of Tutuila.

3.5. Wave systems reconstruction and aggregation

Long-term series of sea state parameters can be reconstructed in shallow water through the radial basis function (RBF) interpolation technique. The RBF technique is typically used to interpolate large sets of scattered data in high-dimensional spaces, as happens with data selected with MDA (Camus et al., 2011a,b). Comparisons of multivariate interpolation schemes over scattered data (Alfeld, 1989; Franke, 1982) identify the RBF method as very suitable in terms of accuracy, flexibility, and computational cost. The method approximates a real-valued function as a linear combination of RBFs. The subset cases at deep water are defined as $X_i = \{T_{pi}, \theta_{pi}, \sigma_i, \gamma_i\}$, and the propagated sea-state is expressed as $D_j = \{H_{sj}, T_{pj}, T_{mj}, \theta_{pj}, \sigma_j\}$. The function to approximate is of the form:

$$RBF(X_i) = p(X_i) + \sum_{j=1}^{M} a_j \Phi\left(\left\|X_i - D_j\right\|\right) \quad (1)$$

where $p(X_i)$ is a linear polynomial with coefficients $b = \{b_0, b_1, \ldots, b_d\}$, being n the data dimension, $\|\cdot\|$ is the Euclidean norm, and Φ are Gaussian functions with ε a parameter specified by the user that controls the shape of the distributions. Here, we use the algorithm proposed by Rippa (1999) to obtain the optimal ϵ parameter. Coefficient a_j and b result from the interpolation condition:

$$RBF(D_j) = f_i(D_j); j = 1, \ldots, M \quad (2)$$

Multidimensional RBF interpolation allows the replacement of the SWAN model to obtain the individual wave partitions downscaled at any location in the domain.

Before the final metamodel setup, a sensitivity analysis on the number of cases (M) has been conducted to determine the optimal subset size. Evenly spaced values have been taken in the range of 100 to 1000. For every classification size M, a k-fold cross-validation procedure has been applied to estimate the skill of the hybrid method MDA-SWAN-RBF to predict K_p at the Apolima buoy location. The cross-validation procedure consists of shuffling the dataset randomly and splitting it into k groups. Each unique group becomes the test set, and the remaining groups are the training dataset. The RBF technique is then fit on the training data and evaluated on the test data. Differences between the predicted and modeled K_p are estimated by the root-mean-square error (RMSE). We decided to divide the dataset into 5 groups ($k = 5$), obtaining the mean and standard deviation of the K_p RMSE for every M classification size (Fig. 4a). The error decreases exponentially with M up to 800 cases, at which point it stabilizes and becomes minimal. Accordingly, for our methodology, the MDA subset size is set to 800.

Concurrent wave systems are aggregated as a linear superposition of wave trains in the spectral band. At a given time, a sea state may be characterized by a wind-sea partition and swell systems (partitions 1 to 5). From the training subset of boundary conditions and their propagation at a certain location, the RBF interpolation permits to obtain K_p, T_p, T_m, θ_p, and σ of each wave system. Every local wave partition H_s is then calculated as the boundary wave partition H_s multiplied by the local K_p. The resulting integral sea state is then computed by the quadratic aggregation of the H_s values of the partitions, whereas the wave period and wave direction are selected from the most energetic partition, where the wave energy is evaluated as $H_s^2 \cdot T_p$. However, the major strength of the method used in this study is that it allows us to reconstruct the directional spectral information in a fast and efficient manner. For this purpose, we use once again the Wavespectra package to construct a JONSWAP-type spectrum from the parameters H_s, T_p, θ_p, σ, and γ of every wave partition. At a specific location, we can obtain from the MDA-SWAN-RBF metamodel the hourly structure of the parameterized wave systems. Every wave system is then translated into a JONSWAP spectrum, and the aggregated spectra is computed as the linear summation of the spectral energy density.

4. Results

4.1. Validation

The capability of HyWaves to reconstruct long-term wave series has been evaluated using instrumental data in Samoa, American Samoa,

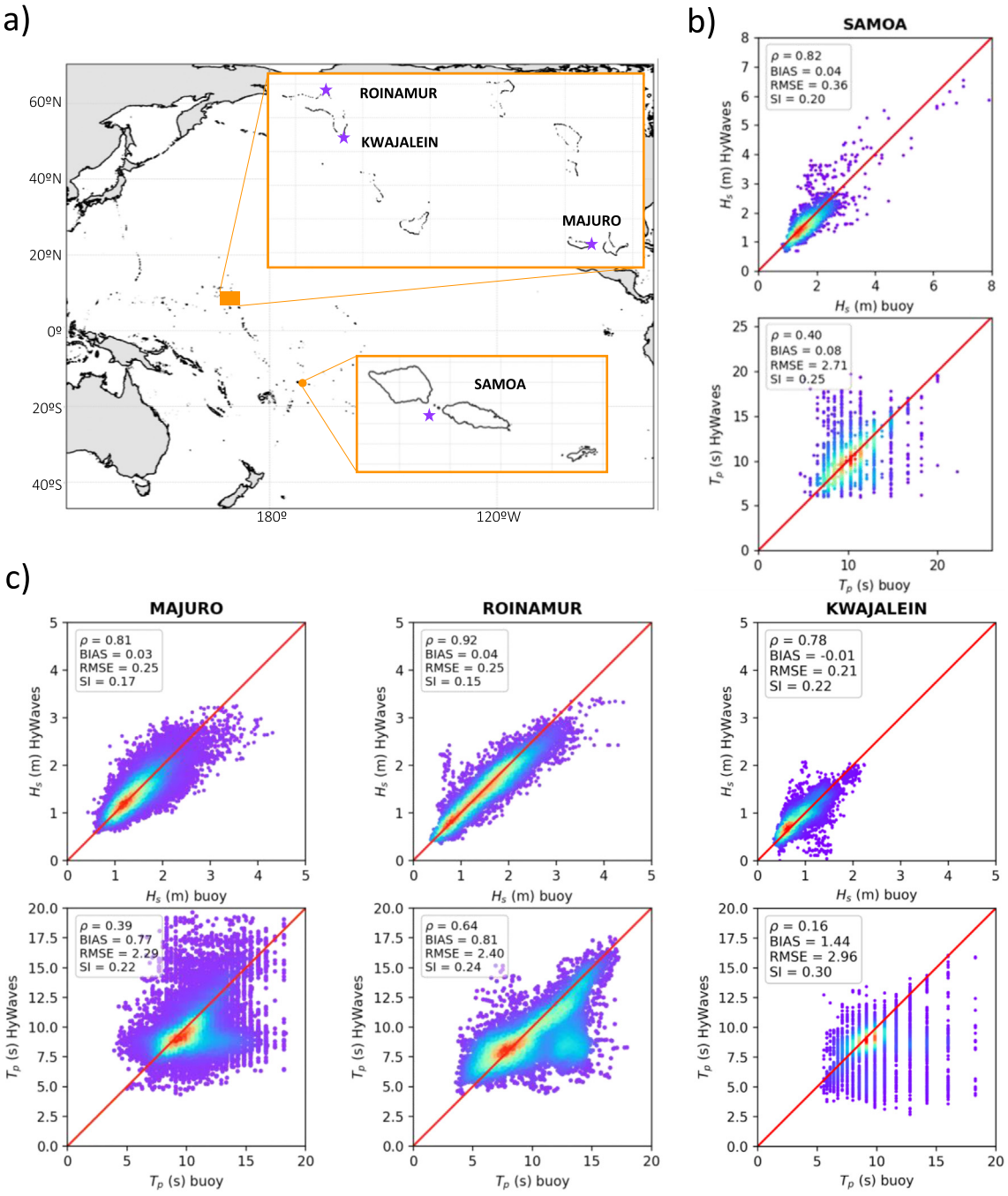

Fig. 5. Study sites validation: (a) Location of the study site islands in the western Pacific. A magenta box surrounds the computational domains, and stars indicate where the buoys used for validation in (b) and (c) are located. (b) Density scatters of the measured wave height and wave period against reconstructed HyWaves output at the Apolima buoy. (c) Scatter diagrams for Majuro, Roi-Namur, and Kwajalein study sites.

Majuro, and in the north and south of Kwajalein Atoll. The location of the study sites in the western Pacific and their computational domains are presented in Fig. 5; a comparison of the measured wave height and wave period against the HyWaves methodology results are shown in Fig. 5b and 5c. Some diagnostic metrics are listed on the plots to directly measure the accuracy of the method, such as Pearson's correlation coefficient (ρ), *RMSE*, the systematic deviation between two random variables (*BIAS*) and the residual scatter index (*SI*). HyWaves predicts the H_s accurately in all depths with biases that are consistently close to zero. The best result in terms of H_s prediction was observed in Roi-Namur with the highest correlation coefficient (ρ = 0.92). The accuracy of the reconstructed parameters is notably worse for wave period. *SI* related to T_p are below 0.25, *RMSE* below 2.5, and ρ between 0.39 and 0.64. The performance of the hybrid metamodel in Kwajalein is significantly worse than in the rest of the study sites. This can be explained by the poor quality of the bathymetric data in a complex curving reef system, and a lower level of accuracy of the measurement method (in this case pressure loggers versus the buoys used in Samoa and Majuro), that can also affect the conclusions taken about model performance. In our study, we do not have other measurements to compare the error introduced during the wave measurement. However, previous experiments such as the ones performed by Andrews and Peach (2019), and Lancaster et al. (2021), show an underestimation of the significant wave height (by 5–7%), and overestimation of the mean wave period (by 18%–27%) when comparing wave parameter recorded by pressure loggers to Spotter o RDI ADCP measurements in Australia.

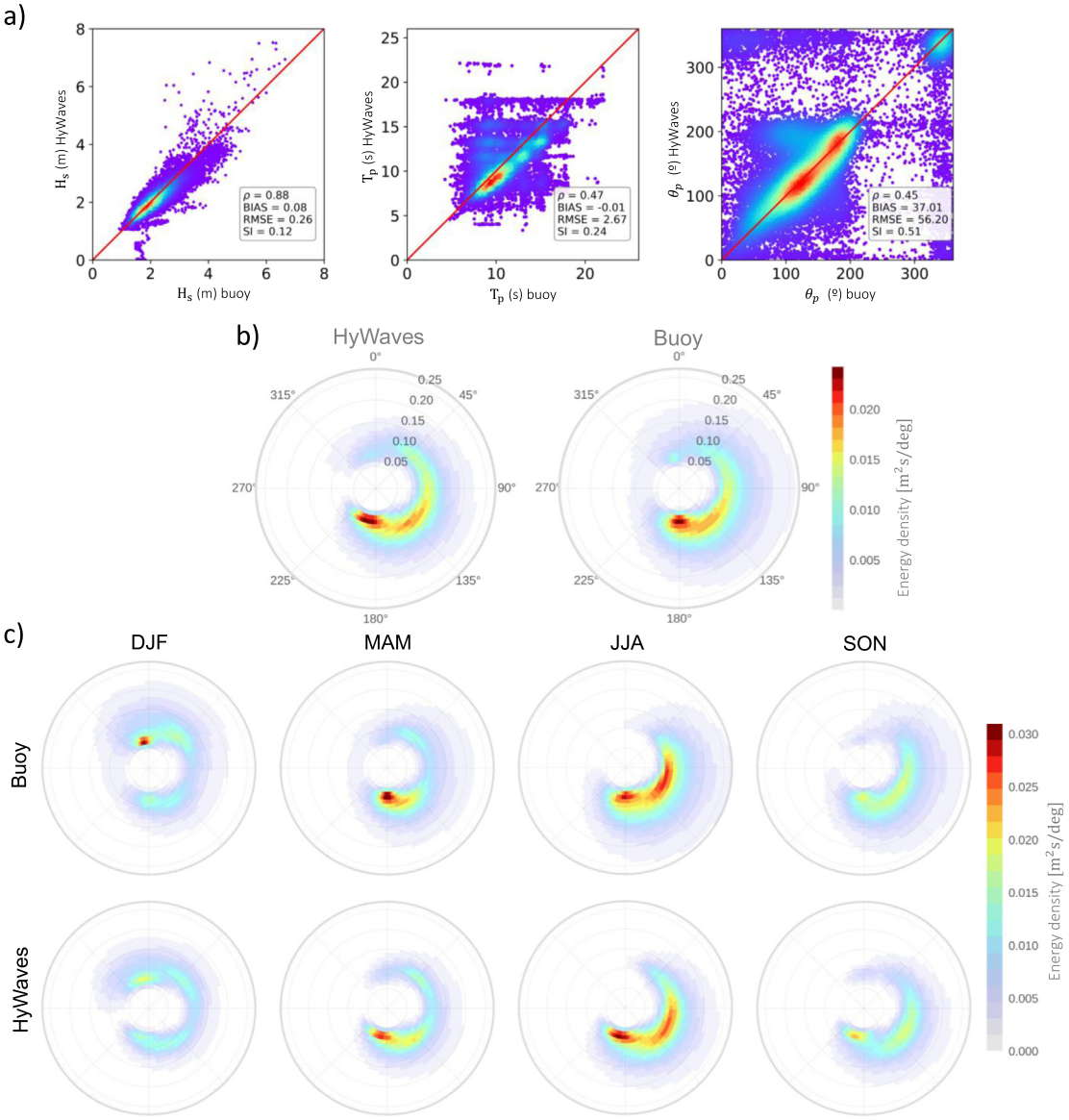

Fig. 6. Spectral validation at Aunu's Buoy. (a) Scatter diagrams of measured versus modeled H_s, T_p and θ_p. (b) Averaged wave energy spectra reconstructed by HyWaves and measured by the buoy. Colors represent the variance spectral density. (c) Comparison of averaged seasonal wave spectra from HyWaves and the buoy. The seasons correspond to December–January–February (DJF), March–April–May (MAM), June–July–August (JJA), and September–October–November (SON).

Furthermore, the validation of the bulk parameters of the Aunu'u buoy, whose location is displayed in Fig. 1a, is presented in Fig. 6a. Although this buoy is anchored in intermediate waters and nonlinear processes may become significant, HyWaves reconstructs the bulk parameters H_s, T_p and θ_p quite accurately. In the T_p scatter diagram, a second density area centered on the 10 s measured by the buoy can be observed. This can be associated with an erratic behavior of the T_p measured by the buoy and noticeable in the Aunu'u time series of the variable. Moreover, we have evaluated the ability of HyWaves to obtain a spectral wave climate characterization at the Aunu'u wave buoy. The 8-year measuring period of the buoy has been reconstructed using HyWaves and compared to the spectral conditions measured by the buoy. The average wave spectra of HyWaves versus the buoy are presented in Fig. 6b and 6c. The spectral patterns found in the reconstruction are qualitatively consistent with the ones measured by the buoy, although the direction of the highest energetic southern swells is slightly rotated south compared with the buoy.

To have an insight into the seasonal variability of the different wave systems picked up by the buoy and reconstructed by HyWaves, the averaged seasonal wave spectra are presented in Fig. 6c. In the austral winter (June–August), the storms in the Southern Ocean generate long-period swells arriving in Tutuila Island from South and Southeast directions. The energy of these swells greatly decays during the months of September, October, and November. In turn, during the boreal winter (December–February) north Pacific storms produce swells that approach the Aunu'u buoy by the north. During the JJA and SON months, higher frequency peaks are recorded from eastern directions related to the contribution of the trade winds to the wave spectra. Nevertheless, the overall consistency gives confidence in the robustness of the methodology proposed.

In addition, the accuracy of the HyWaves reconstruction has been tested against the dynamical downscaling approach by feeding SWAN with hourly non-stationary spectral wave data from the Super-point. Two months have been picked out from the available buoy period. The first month (15 Oct 1989–15 Nov 1989) corresponds to average wave climate conditions and the second month (01 Mar 1990–01 Apr 1990) includes a moderate wave event with a maximum H_s of 4 m in response to the passage of the Tropical Cyclone Rae through the South.

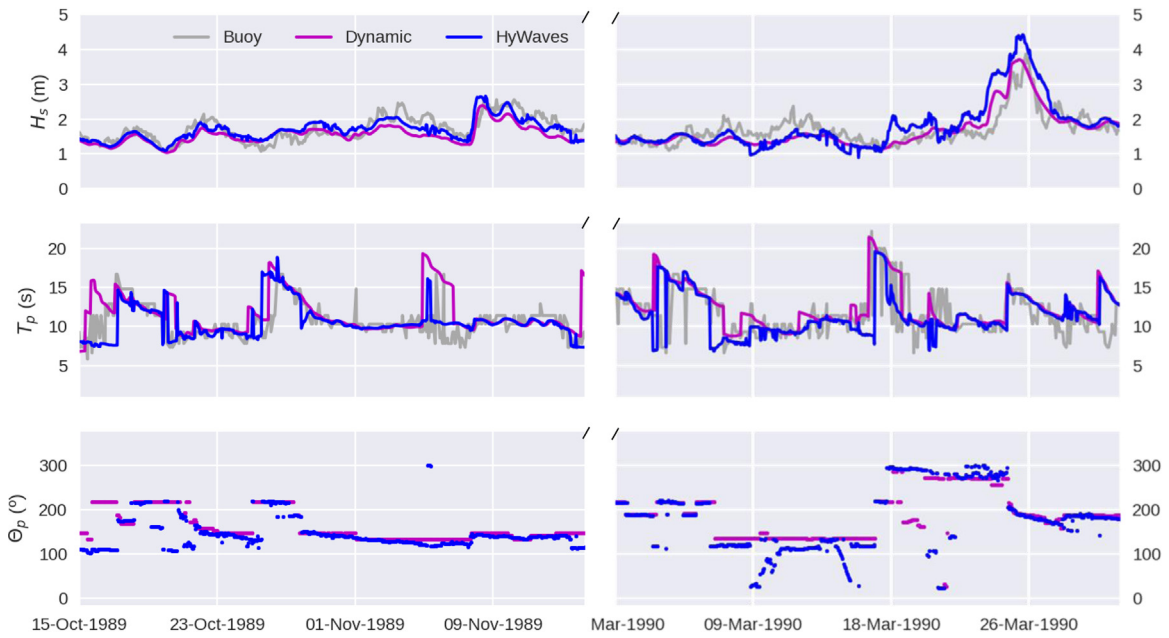

Fig. 7. Comparison between measured and model H_s, T_p, θ_p at the Apolima Buoy (in gray) given by HyWaves metamodel (in blue) and the spectral non-stationary simulation (in magenta).

The comparison of both approaches against the hourly wave parameters recorded by the Apolima Buoy are provided in Fig. 7. The event on 26 March 1990 is slightly overestimated in H_s by HyWaves and better modeled by the non-stationary approach. However, the buoy record and both model-based approaches are found to have a similarly good agreement for the rest of the period. The full dataset of 800 cases and the two months of non-stationary simulation took 2 days on the same computer to run. The operating system employed is Ubuntu (x86-64), using up to eight 3 GHz Intel i7-9700 processors and 32 GB of RAM. The 2 months were later reconstructed in less than a minute and the entire 40-years historical dataset in approximately 5 minutes. This analysis highlights that dynamic modeling can also present discrepancies with the buoy record while HyWaves presents comparable accuracy at a far reduced computing cost.

5. Conclusions

In this study, a new hybrid methodology for downscaling spectrally multimodal wave fields to coastal areas, termed HyWaves, is presented. Long-time series of offshore spectral wave conditions must be used as training data, such as (as in this study) historical wave hindcasts. The hybrid wave transformation model combines statistical and numerical methods to replace the highly computationally expensive method of solely spectral dynamical downscaling. Instead of numerically downscaling several decades of hindcast records, HyWaves allows the efficient reconstruction of wave conditions at any point of the domain, based on, in the case presented here, just 800 stationary wave simulations. The MDA algorithm allows optimizing the number of cases to be run by the nearshore spectral wave propagation model SWAN to use the RBF interpolation technique for the reconstruction of individual wave partitions. Relying on the assumption of wave linear theory allows rescaling of the unitary wave systems and to linearly aggregate the reconstructed concurrent wave systems. However, this assumption may be violated when higher non-linearities due to wave–wave interaction and wave breaking play an important role in wave transformation processes. In the intra-Pacific Islands of our study, the very steep insular reef formations permit the assumption of linearity in the rescaling and aggregation of unimodal SWAN simulations to locations very close to the coast. Nonetheless, in shallow waters, wave celerity (and thus shoaling) is increasingly governed by water depth, and wave breaking by water depth/wave height ratios, and thus the linear solution proposed in this study is not warranted. Another non-linear key process in the modeling is the local wind generation. The domains enclosing the oceanic islands presented in this study are relatively small and the local wind generation can be assumed negligible. A different approach must be used for downscaling wave climate in regions with considerable local wind forcing since stationary simulations could overestimate the wind field. For these reasons, we use HyWaves to downscale wave climate to deep-to-intermediate waters without considering the wind effect. Meanwhile, further research is being done to propose new downscaling methods valid for shallow, non-linear wave dynamics.

The ability of the hybrid method to reproduce the time series of integral wave parameters in coastal areas has been tested against buoy data and compared to dynamical downscaling. Comparison between both approaches has proved to be similar and a positive validation with measured data has been found. Furthermore, the capacity of HyWaves to reconstruct long-term spectral wave conditions has been compared to wave spectra measured by the buoy, finding an overall good agreement in the energy distribution along frequencies and directions. Even though HyWaves has been applied at singular locations for validation purposes, the application of the metamodel to evenly spaced locations in the entire domain permits to account for a wide range of time scale spectral analyses (e.g., seasonal and interannual variability). Moreover, downscaling from spectral partitioning allows to easily track the wave systems over space and time and to gain insight into multimodal climatology.

HyWaves is proposed as an efficient approach for transferring multimodal offshore wave conditions to near-shore locations. Once the method is locally trained, the computational effort is minimal. Although in this paper the methodology has been applied to small Pacific Islands (i.e., Samoa, Tutuila, Majuro, and Kwajalein) and forced with hindcast wind-wave data, it could also be extended to larger spatial scales and to emulated time series, such as developed in Cagigal et al. (2021). In this way, the methodology can potentially facilitate the integration of the effects of climate change in the occurrence and intensity of distant storms and their effect on the nearshore wave climate. In the short term, the use of HyWaves as a modeling tool integrated into EWS can help to accelerate our response to coastal flooding. Ultimately, this methodology advances research in proving an

efficient tool for supporting the detection of natural hazards and related disasters by effectively accelerating our ability to make predictions without sacrificing much skill.

CRediT authorship contribution statement

Alba Ricondo: Methodology, Formal analysis, Software, Visualization, Writing – original draft. **Laura Cagigal:** Methodology, Software, Writing – review & editing. **Ana Rueda:** Conceptualization, Writing – review & editing. **Ron Hoeke:** Conceptualization, Writing – review & editing. **Curt D. Storlazzi:** Resources, Writing – review & editing. **Fernando J. Méndez:** Methodology, Conceptualization, Supervision, Writing – review & editing, Funding acquisition.

Declaration of competing interest

The authors declare that they have no known competing financial interests or personal relationships that could have appeared to influence the work reported in this paper.

Data availability

Data will be made available on request.

Acknowledgments

This work would not have been possible without funding from the Spanish Ministry of Science and Innovation, project Beach4cast PID2019-107053RB-I00. The authors would like to acknowledge CSIRO, for making the spectral hindcast data publicly available, PacIOOS (www.pacioos.org), part of the U.S. Integrated Ocean Observing System (IOOS®), for providing the Kalo and Aunu'u wave buoy measurements, the U.S. Geological Survey (www.sciencebase.gov) for providing the Kwajalein and Roi-Namur field observations, and Oceanor-SOPAC (today Fugro-SPC) for the Apolima buoy data. LC acknowledges the funding from the Juan de la Cierva – Formación FJC2021-046933-I/ MCIN/ AEI/ 10.13039/501100011033 and the European Union "NextGenerationEU"/ PRTR. ARu acknowledges the funding from the Juan de la Cierva-Incorporación IJC2020-043907-I/ MCIN/AEI/ 10.13039/5011 00011033 and the European Union "NextGenerationEU"/PRTR. ARi is funded by a Concepción Arenal studentship from the Universidad de Cantabria. We thank Kai Parker for conducting a USGS internal review of this manuscript. Any use of trade, firm, or product names is for descriptive purposes only and does not imply endorsement by the U.S. Government. I understand that any modifications made to a published article require careful consideration and adherence to the journal's policies. Therefore, I kindly request your guidance on the appropriate procedure to follow for making this minor modification. I am more than willing to provide any necessary documentation or clarification to support this request.

References

Alfeld, P., 1989. Scattered data interpolation in three or more variables. In: Mathematical Methods in Computer Aided Geometric Design, Vol. 5. Academic Press, Inc., http://dx.doi.org/10.1016/b978-0-12-460515-2.50005-6.

Anderson, D.L., Ruggiero, P., Mendez, F.J., Barnard, P.L., Erikson, L.H., O'Neill, A.C., Merrifield, M., Rueda, A., Cagigal, L., Marra, J., 2021. Projecting climate dependent coastal flood risk with a hybrid statistical dynamical model. Earth's Future 9 (12), http://dx.doi.org/10.1029/2021EF002285, e2021EF002285.

Andrews, E., Peach, L., 2019. Wave Monitoring Equipment Comparison: An Evaluation of Current and Emerging in-Situ Ocean Wave Monitoring Technology. Queensland Dept. of Environment and Science Coastal Impacts Unit Publ., p. 63.

Barstow, S., Haug, O., 1994. The Wave Climate of Western Samoa. South Pacific Applied Geoscience Commission, SOPAC Tech, 25.

Booij, N., Ris, R.C., Holthuijsen, L.H., 1999. A third-generation wave model for coastal regions: 1. Model description and validation. J. Geophys. Res. 104 (C4), 7649–7666. http://dx.doi.org/10.1029/98JC02622.

Cagigal, L., Rueda, A., Ricondo, A., Pérez, J., Ripoll, N., Coco, G., Méndez, F.J., 2021. Climate-based emulator of distant swell trains and local seas approaching a pacific atoll. J. Geophys. Res.: Oceans 126 (6), http://dx.doi.org/10.1029/2020JC016919.

Camus, P., Mendez, F.J., Medina, R., 2011a. A hybrid efficient method to downscale wave climate to coastal areas. Coast. Eng. 58 (9), 851–862. http://dx.doi.org/10.1016/j.coastaleng.2011.05.007.

Camus, P., Mendez, F.J., Medina, R., Cofiño, A.S., 2011b. Analysis of clustering and selection algorithms for the study of multivariate wave climate. Coast. Eng. 58 (6), 453–462. http://dx.doi.org/10.1016/j.coastaleng.2011.02.003.

Camus, P., Mendez, F.J., Medina, R., Tomas, A., Izaguirre, C., 2013. High resolution downscaled ocean waves (DOW) reanalysis in coastal areas. Coast. Eng. 72, 56–68. http://dx.doi.org/10.1016/j.coastaleng.2012.09.002.

Camus, P., Menéndez, M., Méndez, F.J., Izaguirre, C., Espejo, A., Cánovas, V., Pérez, J., Rueda, A., Losada, I.J., Medina, R., 2014. A weather-type statistical downscaling framework for ocean wave climate. J. Geophys. Res.: Oceans 119 (11), 7389–7405. http://dx.doi.org/10.1002/2014JC010141.

Cheriton, O.M., Storlazzi, C.D., Rosenberger, K.J., 2016. Observations of wave transformation over a fringing coral reef and the importance of low-frequency waves and offshore water levels to runup, overwash, and coastal flooding. J. Geophys. Res. Oceans 121, 3121–3140. http://dx.doi.org/10.1002/2015JC011231.

Cid, A., Camus, P., Castanedo, S., Méndez, F.J., Medina, R., 2017. Global reconstructed daily surge levels from the 20th Century Reanalysis (1871–2010). Glob. Planet. Change 148, 9–21. http://dx.doi.org/10.1016/J.GLOPLACHA.2016.11.006.

Draycott, S., Davey, T., Ingram, D.M., 2017. Simulating extreme directional wave conditions. Energies 10 (11), http://dx.doi.org/10.3390/en10111731.

Ford, M., Merrifield, M.A., Becker, J.M., 2018. Inundation of a low-lying urban atoll island: Majuro, Marshall Islands. Nat. Hazards 91 (3), 1273–1297. http://dx.doi.org/10.1007/s11069-018-3183-5.

Franke, R., 1982. Scattered data interpolation: tests of some method. Math. Comp. 38 (157), 181. http://dx.doi.org/10.2307/2007474.

Genz, J., Aucan, J., Merrifield, M., Finney, B., Joel, K., Kelen, A., 2009. Wave navigation in the Marshall Islands: Comparing indigenous and Western scientific knowledge of the ocean. Oceanography 22 (SPL.ISS. 2), 234–245. http://dx.doi.org/10.5670/oceanog.2009.52.

Gerling, T.W., 1991. In: Beal, R.C. (Ed.), A Comparative Anatomy of the LEWEX Wave Systems. The John Hopkins University Press, pp. 182–193, Directional Ocean Wave Spectra.

Gerling, T.W., 1992. Partitioning sequences and arrays of directional ocean wave spectra into component wave systems. J. Atmos. Ocean. Technol. 9 (4), 444–458. http://dx.doi.org/10.1175/1520-0426(1992)009<0444:psaaod>2.0.co;2.

Goda, Y., 1983. Analysis of wave grouping and spectra of long-travelled swell. Rep. Port Harbour Res. Inst. 22 (1983), 3–41.

Gouldby, B., Méndez, F.J., Guanche, Y., Rueda, A., Mínguez, R., 2014. A methodology for deriving extreme nearshore sea conditions for structural design and flood risk analysis. Coast. Eng. 88, 15–26. http://dx.doi.org/10.1016/J.COASTALENG.2014.01.012.

Hanson, J.L., Phillips, O.M., 2001. Automated analysis of ocean surface directional wave spectra. J. Atmos. Ocean. Technol. 18 (2), 277–293. http://dx.doi.org/10.1175/1520-0426(2001)018<0277:AAOOSD>2.0.CO;2.

Hasselmann, K., Barnett, T.P., Bouws, E., Carlson, H., Cartwright, D.E., Enke, K., Ewing, J.A., Gienapp, H., Hasselmann, D.E., Kruseman, P., Meerburg, A., Müller, P., Olbers, D.J., Richter, K., Sell, W., Walden, H., 1973. Measurements of wind-wave growth and swell decay during the Joint North Sea Wave Project (JONSWAP). Ergänzungsheft 8–12, https://repository.tudelft.nl/islandora/object/uuid%3Af204e188-13b9-49d8-a6dc-4fb7c20562fc.

Hegermiller, C.A., Antolinez, J.A.A., Rueda, A., Camus, P., Perez, J., Erikson, L.H., Barnard, P.L., Mendez, F.J., 2017. A multimodal wave spectrum–based approach for statistical downscaling of local wave climate. J. Phys. Oceanogr. 47 (2), 375–386. http://dx.doi.org/10.1175/JPO-D-16-0191.1.

Hoeke, R.K., Damlamian, H., Aucan, J., Wandres, M., 2021. Severe flooding in the atoll nations of tuvalu and kiribati triggered by a distant tropical cyclone pam. Front. Mar. Sci. 7, 991. http://dx.doi.org/10.3389/FMARS.2020.539646/BIBTEX.

Hoeke, R.K., McInnes, K.L., Kruger, J.C., McNaught, R.J., Hunter, J.R., Smithers, S.G., 2013. Widespread inundation of Pacific islands triggered by distant-source wind-waves. Glob. Planet. Change 108, 128–138. http://dx.doi.org/10.1016/j.gloplacha.2013.06.006.

Holthuijsen, L.H., 2010. Waves in Oceanic and Coastal Waters, Vol. 148. Cambridge University Press, pp. 148–162.

Kruger, J., 2007. Composite bathymetric map of Samoa: Upolu and Savai'i. 1: 250 000 SOPAC Bathymetry Series Map 41.

Lancaster, O., Cossu, R., Boulay, S., Hunter, S., Baldock, T.E., 2021. Comparative wave measurements at a wave energy site with a recently developed low-cost wave buoy (spotter), ADCP, and pressure loggers. J. Atmos. Ocean. Technol. 38 (5), 1019–1033. http://dx.doi.org/10.1175/JTECH-D-20-0168.1.

Palaseanu-Lovejoy, M., Poppenga, S.K., Danielson, J.J., Tyler, D.J., Gesch, D.B., Kottermair, M., Jalandoni, A., Carlson, E., Thatcher, C., Barbee, M., 2018. One-meter topobathymetric digital elevation model for majuro atoll, republic of the marshall islands. U.S. geological survey scientific investigations report 2018-5047. 27, http://dx.doi.org/10.3133/SIR20185047.

Portilla, J., Ocampo-Torres, F.J., Monbaliu, J., 2009. Spectral partitioning and identification of wind sea and swell. J. Atmos. Ocean. Technol. 26 (1), 107–122. http://dx.doi.org/10.1175/2008JTECHO609.1.

Portilla-Yandún, J., Cavaleri, L., Van Vledder, G.P., 2015. Wave spectra partitioning and long term statistical distribution. Ocean Model. 96, 148–160. http://dx.doi.org/10.1016/j.ocemod.2015.06.008.

Rajindas, K.P., Shashikala, A.P., 2021. Development of hybrid wave transformation methodology and its application on Kerala Coast, India. J. Earth Syst. Sci. 130 (2), http://dx.doi.org/10.1007/s12040-021-01612-3.

Rippa, S., 1999. An algorithm for selecting a good value for the parameter c in radial basis function interpolation. Adv. Comput. Math. 11 (2), 193–210. http://dx.doi.org/10.1023/A:1018975909870.

Rosenberger, K.J., Cheriton, O.M., Storlazzi, C.D., 2020. Cross-reef wave and water level data from coral reef environments (ver. 2.0, 2021). U.S. Geological Survey Dara Release. http://dx.doi.org/10.5066/P9RYN5NH.

Saha, S., Moorthi, S., Pan, H.L., Wu, X., Wang, J., Nadiga, S., Tripp, P., Kistler, R., Woollen, J., Behringer, D., Liu, H., Stokes, D., Grumbine, R., Gayno, G., Wang, J., Hou, Y.T., Chuang, H.Y., Juang, H.M.H., Sela, J., et al., 2010. The NCEP climate forecast system reanalysis. Bull. Am. Meteorol. Soc. 91 (8), 1015–1058. http://dx.doi.org/10.1175/2010BAMS3001.1.

Saha, S., S, M, S, W, X, W, J, N, S, T, 2011. NCEP Climate Forecast System Version 2 (CFSv2) 6-Hourly Products. Research Data Archive at the National Center for Atmospheric Research, Computational and Information Systems Laboratory.

Smith, G.A., Hemer, M., Greenslade, D., Trenham, C., Zieger, S., Durrant, T., 2020. Global wave hindcast with Australian and Pacific Island Focus: From past to present. Geosci. Data J. May, 1–10. http://dx.doi.org/10.1002/gdj3.104.

Smith, W.H., Sandwell, D.T., 1997. Global sea floor topography from satellite altimetry and ship depth soundings. Science 277, 1956–1962. http://dx.doi.org/10.1126/science.277.5334.1956.

Storlazzi, C.D., Gingerich, S.B., Van Dongeren, A., Cheriton, O.M., Swarzenski, P.W., Quataert, E., Voss, C.I., Field, D.W., Annamalai, H., Piniak, G.A., McCall, R., 2018. Most atolls will be uninhabitable by the mid-21st century because of sea-level rise exacerbating wave-driven flooding. Sci. Adv. 4 (4), http://dx.doi.org/10.1126/sciadv.aap9741.

Wandres, M., Aucan, J., Espejo, A., Jackson, N., De Ramon N'Yeurt, A., Damlamian, H., 2020. Distant-source swells cause coastal inundation on fiji's coral coast. Front. Mar. Sci. 7 (July), http://dx.doi.org/10.3389/fmars.2020.00546.

Winter, G., Storlazzi, C., Vitousek, S., van Dongeren, A., McCall, R., Hoeke, R., Skirving, W., Marra, J., Reyns, J., Aucan, J., Widlansky, M., Becker, J., Perry, C., Masselink, G., Lowe, R., Ford, M., Pomeroy, A., Mendez, F., Rueda, A., Wandres, M., 2020. Steps to develop early warning systems and future scenarios of storm wave-driven flooding along coral reef-lined coasts. Front. Mar. Sci. 7 (March), 1–8. http://dx.doi.org/10.3389/fmars.2020.00199.